PERGAMON

Renewable Energy 27 (2002) 319–336

RENEWABLE ENERGY

www.elsevier.com/locate/renene

Technical note

# On the transient thermal behaviour of structural walls—the combined effect of time varying solar radiation and ambient temperature

P.T. Tsilingiris

*Department of Energy Engineering, Technological Education Institution (TEI) of Athens, A.Spyridonos str. GR 122 10, Egaleo, Athens, Greece*

Received 6 August 2001; accepted 28 August 2001

**Abstract**

The aim of the present work is to investigate the transient conduction heat transfer in structural walls. The developed finite difference numerical simulation code, which is suitable to run in conventional microcomputers, has the flexibility to incorporate a wide range of boundary and initial conditions and time-dependent forcing functions for the investigation of the transient heat transfer in walls of any design. The analysis was employed for the prediction of the dynamic thermal behaviour of two wall designs under the effect of a step temperature change and a combined time varying ambient temperature and solar radiation corresponding to typical local weather conditions. The results allow the prediction of the transient duration, the transient temperature fields as well as the quasi-steady state heat fluxes. They also allow the investigation of the dynamic effects of realistic time varying meteorological forcing functions and the strong influence of the wall surface absorptivity, something which confirms its importance as a handy instruction and research tool in the renewable and rational use of energy fields. 

## 1. Introduction

The development of heat transfer analysis for the prediction of the thermal behaviour of structural walls is a problem of a fundamental concern in a broad range of engineering applications such as H-V-A-C systems, estimation of heating and cooling loads in buildings as well as in passive solar design. The study of conduction heat transfer aims basically to the solution of the general second order, partial differential equation of heat conduction. Although this mathematical problem has previously been covered in considerable detail [1], analytical solutions are generally difficult to

0960-1481/02/$ - see front matter 
PII: S0960-1481(01)00167-7

**Nomenclature**

| | |
|---|---|
| $a$ | thermal diffusivity ($m^2/s$) |
| $c$ | specific heat capacity (J/kg K) |
| $h$ | heat transfer coefficient ($W/m^2$ K) |
| $I$ | incident solar radiation ($W/m^2$) |
| $k$ | thermal conductivity (W/m K) |
| $L$ | wall thickness (m) |
| $\dot{Q}$ | distributed heat source ($W/m^3$) |
| $q$ | heat flux rate ($W/m^2$) |
| $t$ | time (s) |
| $T$ | temperature (C) |
| $x$ | space coordinate (m) |

*Greeks*

| | |
|---|---|
| $\alpha$ | wall surface absorptivity (-) |
| $\delta$ | wall sublayer thickness (m) |
| $\Delta T$ | time step (s) |
| $\Delta x$ | space step (m) |
| $\rho$ | density ($kg/m^3$) |

*Subscripts*

| | |
|---|---|
| c | composite |
| ci | convective, inner surface |
| co | convective, outer surface |
| eq | equivalent |
| sc | steady-state composite |
| su | steady-state uniform |
| R | room |
| ri | radiative, inner surface |
| ro | radiative, outer surface |
| u | uniform |

obtain. The necessity for obtaining approximate solutions has motivated substantial efforts towards developing numerical methods, among which the finite difference has attracted a considerable attention, primarily because the method is easily adapted to digital computations and contemporary computer hardware [2,3]. Various other

methods have appeared in the literature for the analysis of the conduction heat transfer in buildings like those based on electrical network theory, which allowed the investigation of various design parameters on the thermal behaviour of structural elements for solar passive design applications [4–7]. A thermal equilibrium parametric analysis was developed by Athanassouli and Massouros [8] for the investigation of radiative effects on the heat gain of a uniform wall, while a finite difference model was employed for the investigation of the deviation effects of outdoor air temperature periodicity on a wall heat gain by Antonopoulos and Democritou [9].

The present analysis has allowed the development of a simple and flexible generalised handy microcomputer simulation model, suitable for the investigation of the effects of time varying meteorological forcing functions on the transient thermal behaviour of any structural wall design. The numerical code was developed as a simple and handy research, instruction and design tool for a wide range of load control and passive solar design applications.

## 2. The mathematical formulation

The governing conduction heat transfer equation in an anisotropic medium is

$$\nabla \cdot k \nabla T + \dot{Q} = \rho c(\partial T/\partial t) \tag{1}$$

where $\dot{Q}$ is the distributed thermal source per unit volume and $k$ is the thermal conductivity taken as dependent on the temperature and location.

For a wall of large lateral dimensions compared to its thickness, the conduction heat flow in a direction perpendicular to the wall surface can be treated as one dimensional and for systems without distributed thermal sources the above equation becomes

$$\frac{\partial}{\partial x}\left(k\frac{\partial T}{\partial x}\right) = \rho c \frac{\partial T}{\partial x}, \tag{2}$$

This is a partial differential equation of parabolic form, in which the thermophysical properties $k$, $\rho$ and $c$ are allowed to vary with the coordinate $x$. Assuming that the coordinate system is placed at the external wall surface of a thickness $L$, separating a space at an indoor temperature $T_i(t)$ and the environment at the temperature $T_o(t)$, the boundary conditions of the problem are expressed in terms of the temperature gradient at the wall surfaces

$$q(0,t) = -k(\partial T/\partial x)|_{x=0}, \tag{3}$$

and

$$q(D,t) = -k(\partial T/\partial x)|_{x=L} \tag{4}$$

Assuming that both wall surfaces are exchanging heat with the internal space and

the environment throughout convection and radiation and that the external wall surface is exposed to the incident solar radiation, the above transport quantities $q(0,t)$ and $q(L,t)$ can be expressed as

$$q(0,t) = \alpha I_s(t) + (h_{co} + h_{ro})[T_o(t) - T(0,t)] \quad (5)$$

$$q(L,t) = (h_{ci} + h_{ri})[T(L,t) - T_i(t)] \quad (6)$$

with $h_{co}$ , $h_{ci}$ and $h_{ri}$, $h_{ro}$ the convective and radiative heat transfer coefficients for both the ambient and air-conditioned wall sides, respectively, and $\alpha$ the total hemispherical absorptivity of the external wall surface.

Once the two boundary conditions and an initial condition are specified, solutions of Eq. (2) can be derived analytically, employing various available techiques, such as Laplace transforms, separation of variables or others. However, since exact solutions for such heat conduction problems characterised by time-dependent heat fluxes and temperature fields are generally difficult to obtain, the use of the finite difference method for the derivation of approximate solutions was employed as it is easily adaptive to contemporary powerful microcomputers.

## 3. The development of numerical model

For the application of this method the composite wall was subdivided into sublayer sections of uniform temperature and thermophysical properties, at the centre of which a node of a thermal network was located. A system of simultaneous algebraic equations was then developed by translating the differential equation (2) and the boundary conditions Eqs. (5) and (6) into a set of simultaneous algebraic equations corresponding to each inner and boundary nodes, using the always inherently stable Laasonen implicit finite difference scheme [2,10]. The number of simultaneous equations is proportional to the number of wall sublayer sections and the number of the thermal network nodes.

The specified time domain is also subdivided in a large number of time steps and the solution of the set of simultaneous equations is carried out repeatedly throughout the whole number of integration time steps. The accuracy of calculations improves and the numerical results are converging into exact analytical solutions as soon as the number of time steps, the number of sublayer sections and the thermal network nodes increase. However, excessive increase of sublayer sections and time steps may possibly lead to prohibitively lengthy computer simulation runs and large computer CPU time, especially when working on conventional microcomputers. Therefore the proper optimum selection of the wall sublayer number and time steps is crucial, depending entirely on a compromise between computer CPU time and the accuracy level of calculations. In the present investigation this selection was based on extensive numerical experimentation as it is typically shown in Figs. 1 and 2.

For a fixed time step, the effect of a varying space interval on the accuracy of results is shown in Fig. 1, which refers to a composite wall 0.30 m thick. The temperatures at two different distances at 0.04 and 0.14 m from the external wall surface

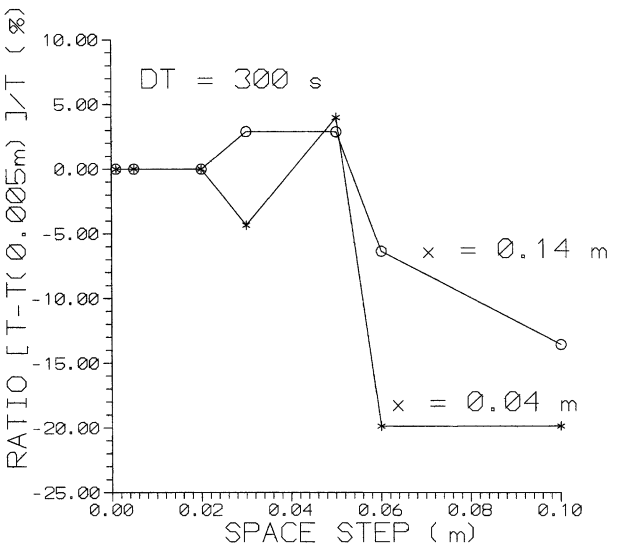


Fig. 1. The effect of the space step selection in the accuracy of the numerical solutions. The dimensionless ratio $[T-T(0.005\ \text{m})]/T$ is plotted as a function of a space interval of 5, 10, 20, 30, 50, 60 and 100 mm for a fixed time step of 300 s and for two fixed locations corresponding to $x$=0.04 and 0.14 m.

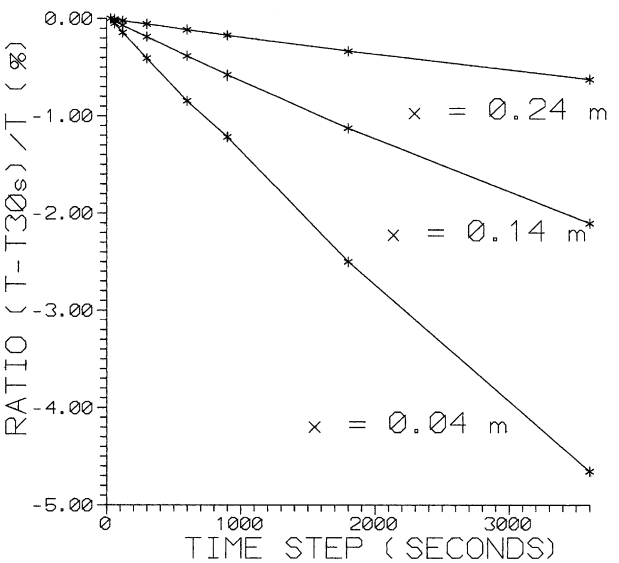


Fig. 2. The effect of the time step selection in the accuracy of the numerical solutions. The dimensionless ratio $[T-T(30\ \text{s})]/T$ is plotted as a function of a time step of 30, 60, 120, 300, 600, 900, 1800 and 3600 s for three fixed locations corresponding to $x$=0.04, 0.14 and 0.24 m.

are calculated at a specified time for a decreasing space interval thickness of 0.1, 0.06, 0.05, 0.03, 0.02, 0.01, and 0.005 m corresponding to 4, 6, 7, 11, 16, 31 and 61 thermal network nodes. The calculated results corresponding to a decreasing sublayer thickness are compared with those corresponding to the finest subdivision of $\Delta x$=5 mm and they are plotted in terms of the (%) ratio of the quantity $(1-T^*/T)$, where $T^*$ and $T$ are the solutions corresponding to the minimum space interval of $\Delta x$=5 mm and any other space interval, respectively.

It is clearly shown that a very coarse subdivision of layers may dramatically deteriorate the accuracy of derived results. More specifically, differences as high as about 20 and 14%, respectively, may be expected at the two fixed locations using a coarse subdivision corresponding to $\Delta x$=0.1 m. The differences are decreasing for a corresponding decrease of sublayer thickness, so as for very fine nodal grids, typically for $\Delta x \leq 2$ cm, the calculated temperatures differ less than 0.01% from those corresponding to the finest space mesh of $\Delta x$=5 mm. For this reason the subsequent numerical calculations were carried out for a $\Delta x$=1 cm.

The optimum selection of the time step $\Delta t$ for simulations was based on similar considerations. The temperatures corresponding to three fixed locations at 0.04, 0.14 and 0.24 m from the external wall surface were calculated for a fixed $\Delta x$=1 cm and for a decreasing time interval of 3600, 1800, 900, 600, 300, 120, 60, and 30 s. The results were compared with those corresponding to the shortest time interval of $\Delta t$=30 s and were plotted in Fig. 2 in terms of the (%) ratio of the quantity $(1-T_{30}/T)$, where $T_{30}$ and $T$ are the calculated solutions corresponding to the minimum time interval of $\Delta t$=30 s and to any other time interval, respectively.

Although the selection of large time intervals may lead to significant decrease of computer CPU time, it may also be responsible for up to 5% deviations from the solutions corresponding to the finest time step of 30 s near the wall boundary. Obviously the effect of using fine time steps on accuracy is stronger near the wall boundary as it is shown in Fig. 2. It is clear from the same plot that for $\Delta t \leq 300$ s, the temperature deviation from those corresponding to the finest time interval of $\Delta t$=30 s, is less than 0.5%. For this reason most of the subsequent numerical calculations were carried out using a space interval of $\Delta x$=1 cm and time steps $\Delta t$ between 60 and 300 s depending on the available computer hardware.

Alternative comparative computer calculations were subsequently also carried out using the same space and time intervals and the Crank-Nicholson finite difference approximation. The differences were found to be always negligible.

A computer simulation code was developed for the solution of the simultaneous equations during each time step $\Delta t$ over the entire time domain of integration, using the triangular factorisation method. The code offers the flexibility of using user defined time and space intervals and sets of various thermophysical properties for the composite wall sublayer materials. It also allows the incorporation of various user selectable initial and boundary conditions like convective, or combined convective and radiative with partial absorption of solar radiation components corresponding to any user defined forcing functions and boundary conditions.

However, referring to conditions when the model simulates a conventional sunlit structural wall element, the variables $I_s(t)$ and $T_o(t)$ appearing in the expressions

Eqs. (5) and (6) represent the meteorological time-dependent forcing functions to the boundary conditions. More specifically while $T_i(t)$ represents the indoor space temperature, $I_s(t)$ is the instantaneous incident solar radiation flux at a vertical wall surface of any azimuth angle or on a horizontal surface and the ambient temperature $T_o(t)$ is expressed in the form of harmonic functions. Since the selection of the appropriate meteorological time-dependent forcing functions is important for the realistic prediction of the wall thermal behaviour under typical weather conditions, long-term local meteorological data were employed.

Easily accessible daily average, statistically treated incident solar radiation data for the Athens area were introduced in the model and a subroutine was developed for the calculation of the corresponding instantaneous data at the wall surface for any desired number of sequential days during the year, according to well-established procedures [11]. Long-term daily range and average ambient temperature data were also employed to derive the appropriate time resolution ambient temperature time series for the desired sequence of simulation days, also based on standard procedures as discussed in greater detail in [12].

## 4. The description of the reference walls

Various standard wall designs are currently employed in construction. Although light frame walls are very popular, a wide range of composite walls, making extensive use of heavier materials like masonry, concrete and bricks, are broadly employed locally, the use of which is mainly imposed by regulations and prevailing conditions. For the purpose of the present investigation two reference wall designs were selected on the basis of their substantially different thermal characteristics, which are broadly employed for construction in the mediterranean region.

The first structure corresponds to a plain reinforced concrete wall of uniform thermophysical properties, which is mainly employed in building frameworks. The second is a composite wall of a typical layered structure, made of two layers of brickwork separated by a layer of a polymer foam thermal insulation and covered by two similar layers of plaster at both the inner and outer wall surfaces. Although both walls are supposed to be 0.25 m thick, their design and thermophysical properties differ considerably. The detailed description of wall layer thicknesses and thermophysical properties is comparatively shown in Table 1.

Heat capacity which represents the wall heat storage capability, is expressed as the mass times the specific heat capacity $M\times c_p$, of the wall. Since the ratio of this quantity to the wall volume is numerically equal to the density times specific heat capacity $\rho\times c_p$, for walls with the same thickness and lateral dimensions this product is also indicative of the wall heat storage capability and can directly be evaluated as $\rho\times c_p=2.024\times10^6$ J/m$^3$ K for the uniform wall from the values of Table 1.

The equivalent quantity for a layered wall of the same overall thickness $L$, composed from $n$ parallel layers of thickness $\delta_1,\delta_2,\ldots,\delta_n$, is calculated by the expression

$$(\rho c_p)_{eq} = (1/L)\sum_{i=1}^{n}(\rho_i c_{p_i}\delta_i). \tag{7}$$

Table 1
Thermophysical properties of wall layersColumn widths

| | $k$ (W/m K) | $\rho$ (kg/m$^3$) | $c$ (J/kg K) |
|---|---|---|---|
| 1. Uniform wall ($L$=25 cm) | 1.4 | 2300 | 880 |
| 2. Composite wall ($L$=25 cm) | | | |
| Layer 1 (plaster, $\delta_1$=2 cm) | 1.39 | 2000 | 1085 |
| Layer 2 (bricks, $\delta_2$=9 cm) | 0.60 | 1400 | 880 |
| Layer 3 (thermal insulation $\delta_3$=3 cm) | 0.041 | 40 | 840 |
| Layer 4 (bricks, $\delta_4$=9 cm) | 0.6 | 1400 | 880 |
| Layer 5 (plaster, $\delta_5$=2 cm) | 1.39 | 2000 | 1085 |

For the corresponding thermophysical properties of Table 1 and $n$=5 it is possible to estimate that $(\rho c_p)_{eq} = 1.238\times10^6$ J/m$^3$ K, which means that the heat storage capability of the concrete wall is about 1.63 times higher than that of the layered wall.

The equivalent thermal conductivity of the layered wall can be evaluated by the expression

$$k_{eq} = L/\sum_{i=1}^{n}(\delta_i/k_i). \tag{8}$$

For the corresponding data in Table 1 and $n$=5 it is possible to evaluate that $k_{eq} = 0.235$ W/m K, something which means that the thermal conductivity of the concrete wall is almost six times higher than the corresponding value for the layered wall.

Thermal diffusivity is a very important physical quantity which determines the wall transient thermal behaviour and represents how fast the heat diffuses through the wall material. This quantity can directly be evaluated for the concrete wall by the data of Table 1, as $a = k/\rho c_p = 0.691\times10^{-6}$ m$^2$/s, while the corresponding quantity for the layered wall is $a_{eq} = k_{eq}/(\rho c_p)_{eq} = 0.189\times10^{-6}$ m$^2$/s.

## 5. Results and discussion

The developed analysis was first employed to investigate the transient thermal behaviour of the two reference walls under the effect of a step temperature change. The computer model was next employed to investigate the time-dependent temperature field and the transient as well as the quasi-steady state time varying heat losses for the same walls under the combined effect of a harmonically varying ambient temperature and a time varying flux of incident solar radiation at the outer wall surface.

### 5.1. The influence of step ambient air temperature change

Aiming to investigate the effect of a step ambient and room air temperature change, it was initially assumed that there is no incident solar radiation at the surface of the wall which was considered to be initially isothermal at a uniform temperature of 10°C. At $t$=0, both wall surfaces are exposed to fixed air temperatures which are for the ambient and for the room sides equal to 5°C and 20°C, respectively. For the purpose of the first order calculations the effect of radiative heat exchange was neglected and fixed convective heat transfer coefficients were assumed at both wall surfaces. The integration was carried out for a time domain of five days in order to allow the full investigation of the transient phenomenon as well as the gradual approach to steady-state conditions. The computer model allows the calculation of temperature distribution profiles at 2, 4, 8, 12, 16, 20 and 24 h from $t$=0, which were stored and plotted in Figs. 3 and 4, corresponding to the uniform and the layered walls, respectively.

The vertical displacement between the initial and subsequent successive temperature distributions indicates how rapidly the wall responds to the step change of the ambient air temperature. Except for the first temperature distribution corresponding to 2 h, the temperature profiles for the uniform wall in Fig. 3 appear to be almost linear and closely spaced. This means that the development of strong temperature gradients at the wall boundaries immediately upon the influence of the step air temperature change, is responsible for transient conduction heat fluxes, which very rapidly lead to the development of almost linear temperature distributions, indicating

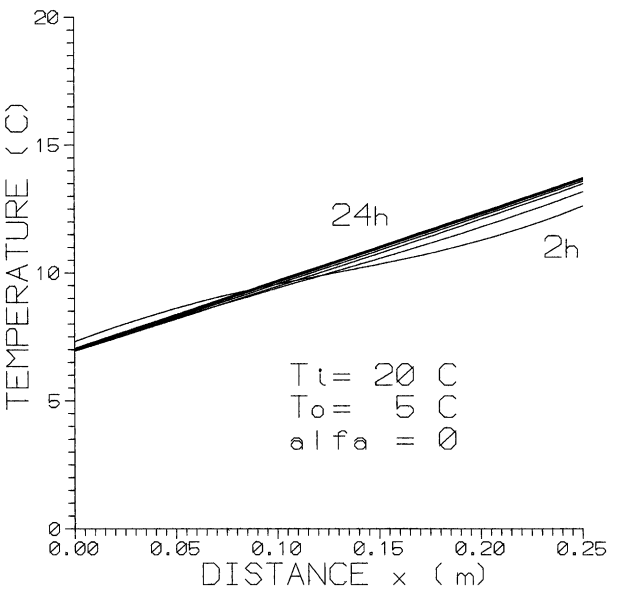


Fig. 3. The developed transient temperature distributions at 2, 4, 8, 12, 16, 20 and 24 h from $t$=0 for the uniform wall when subjected to a step ambient temperature change.

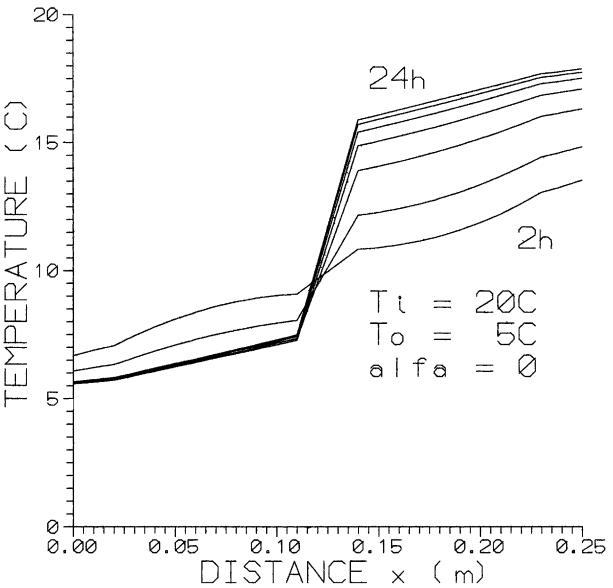


Fig. 4. The developed transient temperature distributions at 2, 4, 8, 12, 16, 20 and 24 h from $t$=0 for the composite wall when subjected to a step ambient temperature change.

conditions close to thermal equilibrium. The latest profiles appear to lie close together owing to the relatively rapid development of the transient, which is followed by an asymptotic approach to the steady-state conditions.

As derived from the last temperature distribution which corresponds closely to thermal equilibrium, the temperature drop across the wall at 24 h is relatively small (only about 7°C) due to the low thermal resistance of the wall, something which leads to a relatively low room wall surface temperature.

The corresponding successive temperature profiles for the composite wall are shown in Fig. 4. Again the development of a transient temperature field immediately upon the influence of the step temperature change, leads to the development of transient temperature gradients and heat fluxes. Now the presence of distinct layers of different thermophysical properties is obvious from the shape of the temperature distributions. The strongest temperature gradients appear to develop near the wall mid-plane where the thermal insulation layer with the lowest thermal conductivity is installed. The local slope of temperature distribution is determined by the corresponding thermal conductivity of wall layer. Owing to the relatively lower equivalent thermal conductivity of the composite wall, the temperature drop across the layered wall is appreciably higher (almost 13°C), something which leads to a proportionally higher room surface temperature.

A comparative inspection of the initial and transient temperature distributions in Figs. 3 and 4 indicates a closer spacing of the corresponding profiles in the uniform wall, something which suggests a more rapid approach to the thermal equilibrium and a shorter duration of the transient.

Although the developed heat fluxes differ appreciably for the two walls, their magnitude after a certain period of time converges to the values predicted by steady-state considerations. This time, which depends on the relative effects of the thermal conductivity and wall heat capacity, can be estimated by plotting the transient heat loss rate over the integration time domain, which allows to determine the asymptotic approach to the thermal equilibrium.

Fig. 5 shows typical simulation results corresponding to the transient thermal behaviour of both walls. The heat flow rates from the room side in ($W/m^2$), are calculated by the expression

$$q(D,t) = h_{ci}[T_R - T(D,t)], \tag{9}$$

where $T_R$ and $T(D,t)$ are the indoor space and wall temperatures.

The results are stored in a data file and they are comparatively plotted in solid lines for both the uniform ($u$) and the composite ($c$) walls. The negative sign signifies the direction of heat flow, which is considered as room heat loss.

The influence of the step temperature change, as can clearly be seen from Fig. 5, causes the immediate development of considerably high transient heat fluxes, as high as about 85 and 57 $W/m^2$ for the uniform and the composite walls, respectively. However, these are rapidly decreasing, allowing an asymptotic approach to their respective steady-state heat loss values. This occurs when all transients have died away and it practically happens at about 40 and 48 h for the uniform and the composite walls, respectively. Therefore the steady-state heat losses can be calculated by the following time average heat loss, for the last 48 h

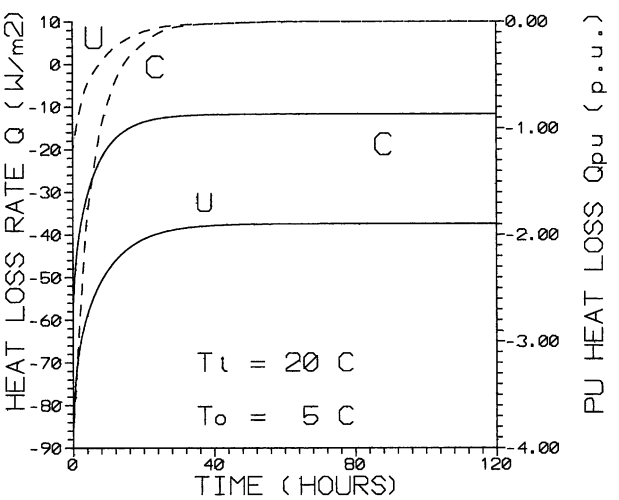


Fig. 5. The transient heat loss rates in ($W/m^2$) for the uniform ($u$) and the composite ($c$) walls (solid lines) during the whole simulation time domain of 120 h. The corresponding dimensionless heat loss rates are shown in broken lines.

$$q = [1/(t_2-t_1)]\int_{t_1}^{t_2} q(t)\,\mathrm{d}t. \tag{10}$$

For $t_1$=72 h and $t_2$=120 h the steady-state heat losses were estimated to be about 37.6 and 11.5 W/m$^2$ for the uniform and the layered walls, respectively. Their appreciable difference is attributed to the remarkably higher thermal resistance of the layered wall, which is responsible for the corresponding dramatic reduction of steady-state heat losses.

These losses were found to be identical to those derived by simple steady state heat conduction considerations, according to the expression

$$q(x = 0) = \Delta T/[1/h_{ci} + \sum_{i=1}^{v} (\delta_i/k_i) + 1/h_{co}], \tag{11}$$

where $\delta_i$ and $k_i$ are the layer thicknesses and thermal conductivities as shown in Table 1 and $\Delta T$=15°C.

Aiming to compare how rapidly the walls respond to the step temperature change, it was found convenient to refer the calculated dimensional heat loss fluxes in their corresponding per unit form owing to their appreciable difference between their steady-state values.

Assuming that $q_{su}$ and $q_{sc}$ represent the steady-state heat loss rates and that $q_u$ and $q_c$ are their corresponding time-dependent values for the composite and uniform walls, the calculated dimensional heat loss rates were converted to the corresponding per unit quantities by the definition of the dimensionless quantities $[q_u(t)-q_{su}]/q_{su}$ and $[q_c(t)-q_{sc}]/q_{sc}$. The numerical value of these ratios, which were plotted in broken lines for both walls, becomes obviously zero for the thermal equilibrium conditions, when $q_u(t)-q_{su}=q_c(t)-q_{sc}=0$.

Comparative inspection of these lines, indicates that the time required for the transient heat loss rates to converge their corresponding thermal equilibrium value is longer for the composite wall. This is attributed to the relative effects of the thermal conductivity $k$, $k_{eq}$ and the heat capacity $\rho\times c_p$ and $(\rho\times c_p)_{eq}$ respectively, which clearly determines the corresponding thermal diffusivity ratio

$$(a/a_{eq}) = 3.65, \tag{12}$$

something which indicates that the heat diffuses more than three times faster in the uniform wall.

### *5.2. The combined influence of time varying driving functions*

The combined influence of the harmonically varying ambient temperature and time varying solar radiation is next investigated on the transient thermal behaviour of walls. Their influence leads to the development of transient temperature fields and time varying heat fluxes, the accurate prediction of which is very important in many

fields of engineering, like space heating load control in air conditioning and passive solar heating design applications. For the provision of the realistic set of local meteorological input driving functions, a special subroutine was developed, which allows the calculation and storage of all the necessary solar insolation and ambient temperature data, both of appropriate time resolution.

Aiming to investigate the effect of the amount of the solar radiation absorption, two fixed values of the total hemispherical absorptivity of the exterior wall surface of $\alpha$=0.2 and 0.8 were considered.

The simulations were first carried out for the uniform wall starting on 20 January for a fixed room temperature of 20°C, employing as initial condition a uniform wall temperature of 10°C.

In Fig. 6 the calculated heat loss rates from the inner wall surface were comparatively plotted in solid lines for $\alpha$=0.2 and 0.8 as a function of time for the 120 simulation hours. In the same plot the calculated incident solar radiation at a south oriented vertical wall, as well as the sinusoidally varying ambient temperatures were also plotted in dotted and dashed lines, respectively.

It is important to note the remarkably high transient heat loss rates during the first simulation steps. These significant heat loss rates as high as 56 W/m$^2$ are identical, irrespective of $\alpha$ within the first about seven hours from $t$=0. However, at sunrise, shortly after seven hours, the heat loss rate of the wall with higher absorptivity decreases appreciably, owing to the comparatively higher radiation absorption and associate heating of the outer wall surface.

Inspection of Fig. 6 also shows that the derived transient wall heat losses are

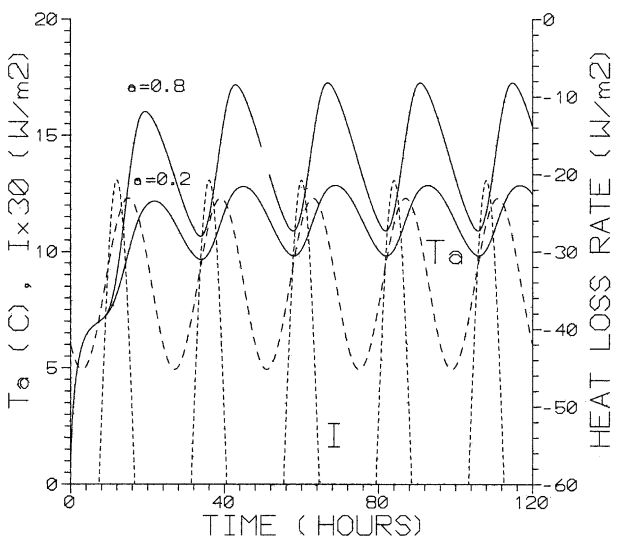


Fig. 6. Prediction of the transient thermal behaviour of the uniform concrete wall under the combined effect of solar radiation and ambient temperature. The transient heat loss rates for $\alpha$=0.2 and 0.8 are plotted in solid lines. The daily variation of ambient temperature and incident solar radiation is plotted in broken and dotted lines, respectively.

rapidly approaching the periodic quasi-steady state behaviour and this practically occurs at about 40 h.

The calculated average value of the quasi-steady state heat loss rate through the expression (10), was found to be 17.69 and 25.72 W/m$^2$ for a wall with a surface absorptivity of $\alpha$=0.8 and 0.2, respectively. This over 30% heat loss reduction indicates the significant effect of radiative properties of sunlit walls for the effective heat loss control in buildings.

It is also important to note that there is a considerable phase lag of about 7 h between the occurrence of maximum solar radiation and minimum heat loss rate for the wall with $\alpha$=0.8, irrespective of transient or quasi-steady state phase. The corresponding time lag for the wall with $\alpha$=0.2 appears to be longer, varying from about 10 h during transient to about 8.5 h during quasi-steady state. At the same time the occurrence of maximum heat losses appears to be in phase irrespective of $\alpha$, since this occurs very much later from the time of sunset.

The development of corresponding transient temperature profiles for the concrete wall is plotted in Fig. 7, in which the wall temperature is plotted against the distance at fixed time intervals of 8, 16 and 24 h from $t$=0, during the first simulation day. There are two temperature profiles for each time interval. The first, in solid line corresponds to $\alpha$=0.2 while the second in broken to $\alpha$=0.8.

From the direct inspection of the first pair of temperature profiles it appears that within the first eight hours, the surface temperature of both walls approaches the

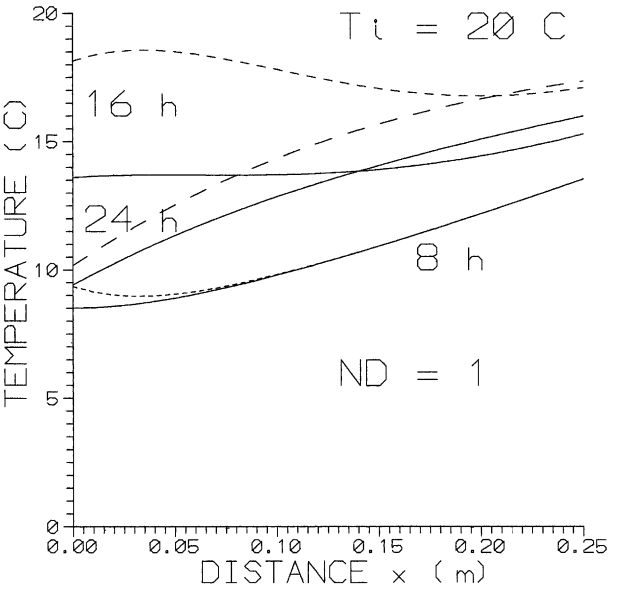


Fig. 7. The developed transient temperature distributions for the uniform wall at 8, 16 and 24 h during the first simulation day (ND=1). The fixed room temperature is $T_i$=20°C while the external wall surface is subjected to the combined effect of solar radiation and ambient temperature. The distributions in solid and broken lines correspond to $\alpha$=0.2 and 0.8, respectively.

respective ambient temperature and a fairly linear temperature distribution develops throughout the wall, except at a region near the outer wall surface. The absorption of incident solar radiation which begins at sunrise, causes the reduction of temperature gradients at the outer wall surface which becomes zero or even negative for $\alpha$=0.2 and 0.8, respectively.

Owing to the combined effects of the maximum incident solar radiation and ambient temperatures which occur slightly earlier, the temperature profiles at 16 h correspond to comparatively higher wall temperatures. At 24 h, relatively stronger temperature gradients are developing at the outer wall surface which lead to corresponding higher heat loss rates from the outer wall, owing to the relatively low ambient temperatures.

The corresponding calculated heat loss rates for the composite wall are plotted with solid lines in Fig. 8, in which the meteorological driving functions are also plotted in broken lines. As in Fig. 6, the effect of the two surface absorptivities of $\alpha$=0.2 and 0.8 is also investigated in the calculated wall heat loss rate.

A qualitatively similar behaviour is exhibited, with the initial development of appreciably high short lived transient heat loss rates, which are rapidly converging to harmonically time varying, quasi-steady state behaviour.

Although maximum transient heat loss rates as high as 58 W/m$^2$ are developed, the wall response to the combined effect of the maximum solar radiation and ambient temperature is appreciably slower, so as the effect of surface absorptivity can only be distinguished not earlier than about 12 h which corresponds to the first solar noon. From this time onwards the wall with the higher surface absorptivity of $\alpha$=0.8

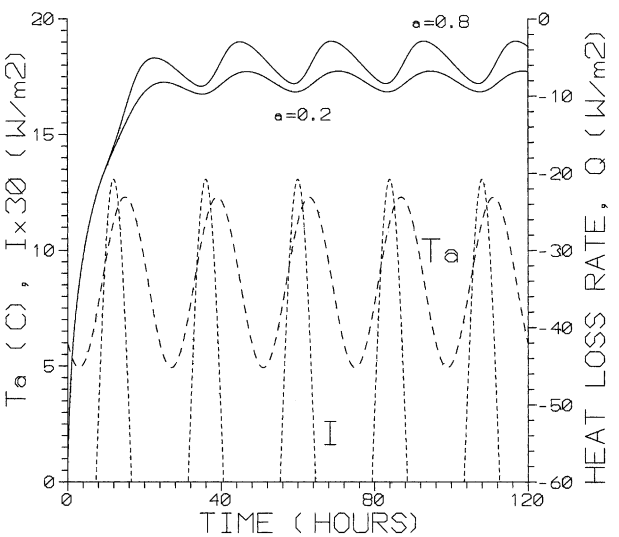


Fig. 8. Prediction of the transient thermal behaviour of the composite wall under the combined effect of solar radiation and ambient temperature. The transient heat loss rates for $\alpha$=0.2 and 0.8 are plotted in solid lines. The daily variation of ambient temperature and incident solar radiation is plotted in broken and dotted lines, respectively.

develops time varying heat loss rates which are lower than the corresponding rates for the wall with $\alpha$=0.2.

The time lag between the occurrence of maximum solar radiation and minimum heat loss rate is now considerably longer, owing to the lower thermal diffusivity of the composite wall. More specifically for $\alpha$=0.8 it is about 11.5 and 8.5 h for the transient and quasi-steady state, respectively, while for $\alpha$=0.2 it is about 13.3 and 11.3 h for the transient and the quasi-steady state, respectively. It is also remarkable to note that the occurrence of the maximum heat losses appears to be in phase for the two walls at solar noon irrespective of $\alpha$.

Comparative inspection of the solid lines in Fig. 8 shows that the transient wall heat loss rates are rapidly approaching the periodic quasi-steady state solutions, the average value of which having been calculated by Eq. (10), was found to be 5.53 and 8.04 W/m$^2$ for surface absorptivities of $\alpha$=0.8 and 0.2, respectively. This corresponds to a significant, over 30% heat loss reduction which can simply be accomplished by the reduction of $\alpha$ with obvious effects on the heat loss control in occupied spaces.

In Fig. 9 the development of transient temperature profiles for the composite wall at the corresponding time intervals of 8, 16 and 24 h from $t$=0 is shown, during the first simulation day. As in Fig. 7, two temperature profiles correspond to each time interval, the first of which in solid line refers to $\alpha$=0.2 while the second in broken line to $\alpha$=0.8.

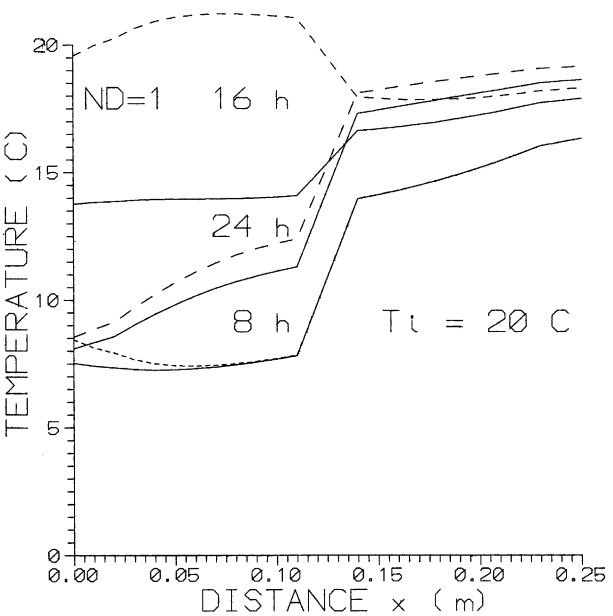


Fig. 9. The developed transient temperature distributions for the composite wall at 8, 16 and 24 h during the first simulation day (ND=1). The fixed room temperature is $T_i$=20°C while the external wall surface is subjected to the combined effect of solar radiation and ambient temperature. The distributions in solid and broken lines correspond to $\alpha$=0.2 and 0.8, respectively.

From the direct inspection of the first pair of temperature profiles it appears that within the first eight hours, both wall surfaces are approaching the respective ambient temperatures and a fairly linear temperature distribution and an almost constant temperature gradient tends to develop throughout the wall, except near the outer surface. Slightly earlier than eight hours, the absorption of solar radiation causes the development of zero or even negative temperature gradients for $\alpha$=0.2 and 0.8, respectively, at the outer wall surface. At 16 h appreciably higher wall temperatures are developed owing to the effects of the peak incident solar radiation and ambient temperatures which occur slightly earlier. An inspection of the temperature distributions near the wall boundaries at 24 h, indicates the development of a substantially stronger temperature gradients at the outer wall surface, something which leads to comparatively higher heat loss rates.

## 6. Conclusions

The purpose of the present analysis was the development of a flexible computer simulation model suitable for the investigation of the dynamic behaviour of structural wall elements, under the effect of time varying driving functions of solar radiation and ambient temperature. Walls are basic construction elements, the transient thermal behaviour of which is an issue of fundamental importance in load control, passive solar design and energy conservation applications. The present computer simulation model which is a handy research and instruction tool, allows the derivation of solutions of the transient heat conduction equation under the appropriate boundary and initial conditions using the finite difference approximation. The thermal behaviour of two wall designs of different characteristics under the influence of a step temperature change and under the combined effect of time varying solar insolation and ambient temperature typical for the mediterranean region was investigated. The analysis has allowed the prediction of the time duration of the transient as well as the comparative calculation of maximum transient and thermal equilibrium wall heat fluxes. The derivation of the temperature distributions and the calculation of the corresponding heat fluxes were also allowed during the transient and the gradual approach to the thermal equilibrium conditions. The transient thermal behaviour of the walls which is strongly influenced by the relative effects of the wall thermophysical properties, was found to be appreciably affected by the surface absorptivity. The value of this important radiative wall property, not only determines the wall dynamic behaviour and the magnitude of the time dependent heat flux but it also affects the phase lag between maximum ambient temperatures and peak heat losses.

## References

[1] Carslaw HS, Jaeger JC. Conduction of heat in solids. Oxford: Clarendon Press, 1959.
[2] Richtmeyer RD. Difference methods for initial-value problems. New York: Interscience, 1957.
[3] Handbook of heat transfer. New York: McGraw-Hill, 1973.

[4] Maloney J, Wang T-C, Chen B, Thorp J. Thermal network predictions of the daily temperature fluctuations in a direct gain room. Sol Energy 1982;29(3):207–23.
[5] Duffin RJ, Knowles G. A passive wall design to minimise building temperature swings. Sol Energy 1984;33(3/4):337–42.
[6] Duffin RJ, Knowles G. Use of layered walls to reduce building temperature swings. Sol Energy 1984;33(6):543–9.
[7] Athieitis AK, Sullivan HF, Hollands KGT. Analytical model, sensitivity analysis and algorithm for temperature swings in direct gain rooms. Sol Energy 1986;36(4):303–12.
[8] Athanassouli G, Massouros G. The influence of solar and long-wave radiation on the thermal gain of a room with opaque external wall. Sol Energy 1983;30(2):161–70.
[9] Antonopoulos KA, Democritou F. On the non-periodic unsteady heat transfer through walls. Int J Energy Res 1993;17:401–12.
[10] Croft DR, Lilley DG. Heat transfer calculations using finite difference equations. London: Applied Science Publishers, 1977.
[11] Duffie JA, Beckmann WA. Solar engineering of thermal processes. New York: Wiley, 1980.
[12] Tsilingiris PT. Solar water heating design — a new simplified dynamic approach. Sol Energy 1996;57(1):19–28.